PLANT SCIENCES

Proteasome-associated ubiquitin ligase relays target plant hormone-specific transcriptional activators

Zhishuo Wang[1], Beatriz Orosa-Puente[1], Mika Nomoto[2], Heather Grey[1], Thomas Potuschak[3], Takakazu Matsuura[4], Izumi C. Mori[4], Yasuomi Tada[2], Pascal Genschik[3], Steven H. Spoel[1]*

The ubiquitin-proteasome system is vital to hormone-mediated developmental and stress responses in plants. Ubiquitin ligases target hormone-specific transcriptional activators (TAs) for degradation, but how TAs are processed by proteasomes remains unknown. We report that in *Arabidopsis*, the salicylic acid– and ethylene-responsive TAs, NPR1 and EIN3, are relayed from pathway-specific ubiquitin ligases to proteasome-associated HECT-type UPL3/4 ligases. Activity and stability of NPR1 were regulated by sequential action of three ubiquitin ligases, including UPL3/4, while proteasome processing of EIN3 required physical handover between ethylene-responsive SCF^{EBF2} and UPL3/4 ligases. Consequently, UPL3/4 controlled extensive hormone-induced developmental and stress-responsive transcriptional programs. Thus, our findings identify unknown ubiquitin ligase relays that terminate with proteasome-associated HECT-type ligases, which may be a universal mechanism for processive degradation of proteasome-targeted TAs and other substrates.

INTRODUCTION

The ubiquitin-proteasome system plays vital roles in regulating cellular homeostasis and responses to the environment in eukaryotes. In plants, developmental and stress response hormones extensively use the ubiquitin-proteasome system to precisely coordinate transcriptional programs (*1*). Several plant hormones have been shown to act as molecular glue between ubiquitin ligases and their substrates (*2*–*4*). This leads to substrate modification by a chain of the small 8-kDa protein ubiquitin that targets substrates to the proteasome for degradation (*5*). Hormone-induced degradation of co-repressors releases the activity of transcriptional activators (TAs), thereby triggering genome-wide transcriptional changes. In addition, hormones control the activities of ubiquitin ligases that directly target TAs to regulate their stability (*6*). For example, ethylene-insensitive 3 (EIN3) is a master TA of the developmental and stress hormone ethylene (*7*). In the absence of ethylene, EIN3 is rapidly targeted to the proteasome by the modular Skp/Cullin/F-box (SCF) ubiquitin E3 ligase, $SCF^{EBF1/2}$, in which EIN3-binding F-box protein 1/2 (EBF1/2) adaptor proteins specifically recruit EIN3 for ubiquitination (*8*–*10*). Thus, when ethylene levels fall, $SCF^{EBF1/2}$ effectively shuts down EIN3-induced transcriptional reprogramming. By contrast, the plant immune hormone salicylic acid (SA) stimulates the stepwise ubiquitination of non-expresser of pathogenesis-related genes 1 (NPR1), a master TA of hundreds of immune genes and promoter of cell survival (*11*–*13*). Initial SA-induced ubiquitination of NPR1 by a Cullin-RING ligase 3 (CRL3) activates NPR1, while subsequent ubiquitin chain elongation by ubiquitin conjugation factor E4 (UBE4) ligase deactivates NPR1 and targets it for degradation (*14*). In addition, SCF^{HOS15} ligase targets NPR1 for degradation to limit and prevent untimely activation of immune genes (*15*). Hence, progressive ubiquitination and subsequent turnover of NPR1 are critical steps in SA-induced immune gene activation.

While the steps leading up to degradation of plant hormone–specific TAs are increasingly well understood, how TAs are shuttled to the proteasome and how the proteasome affects their intrinsic transcriptional activities remain largely unknown. The proteasome itself harbors ubiquitin ligase activity that is thought to be important for promoting proteasome processivity (*16*–*18*). Proteasome-associated ubiquitin ligase activity is conferred by homologous to the E6-AP carboxyl terminus (HECT)–type ubiquitin ligases that directly interact with the 19*S* proteasome subcomplex. Recently, we reported that a member of the *Arabidopsis* HECT-type family of ubiquitin protein ligases (UPLs) not only interacts with the proteasome but, in yeast two-hybrid assays, also is physically associated with hormone-responsive ubiquitin ligases (*19*). Moreover, genetic experiments revealed that UPL1, UPL3, and UPL5 are important for trichome development and SA-induced immunity (*19*, *20*). Thus, UPLs may play an important and yet unrecognized role in proteasome-mediated plant hormone signaling. Here, we show that in *Arabidopsis*, SA- and ethylene-responsive TAs are relayed from pathway-specific ubiquitin ligases to proteasome-associated UPLs, which is necessary for their processive degradation by the proteasome and control of hormone-responsive transcriptional reprogramming.

RESULTS AND DISCUSSION

UPLs endow proteasomes with ubiquitin ligase activity

Little is known about the biochemical activities of UPLs. Therefore, we first assessed the activities of their respective HECT domains in assembling ubiquitin chains. In the presence of the full ubiquitination machinery, HECT domains from all three UPLs successfully formed ubiquitin conjugates, while mutation of the active site cysteine partly compromised their activities (fig. S1A) (*21*). Moreover, like we reported previously for UPL3 (*19*), both the N termini of UPL1 and full-length UPL5 coimmunoprecipitated with 19*S* and 20*S* proteasome subcomplexes in vivo (fig. S1B), suggesting that they interact with the 26*S* proteasome holoenzyme. Therefore, we assessed whether association of all three UPLs endows the proteasome with ubiquitin ligase activity. To that end, we purified fully assembled proteasomes from wild-type (WT) and *upl* mutant plants and

[1]Institute of Molecular Plant Sciences, School of Biological Sciences, University of Edinburgh, Edinburgh, UK. [2]The Centre for Gene Research, Division of Biological Science, Nagoya University, Nagoya, Japan. [3]Institut de Biologie Moléculaire des Plantes, CNRS, Université de Strasbourg, Strasbourg, France. [4]Institute of Plant Science and Resources, Okayama University, Okayama, Japan.
*Corresponding author. Email: steven.spoel@ed.ac.uk

assessed their ability to generate ubiquitin conjugates (fig. S1, C and D). Only proteasomes from immune-induced *upl3* knockout mutants displayed a substantial reduction in proteasome-associated ubiquitin ligase activity (fig. S1D), indicating that, at least in vitro, UPL3 is the primary active ligase. Nonetheless, *upl1*, *upl3*, and *upl5* mutants all displayed decreased cellular levels of ubiquitin conjugates and polyubiquitination of the model substrate RPN10 (fig. S1E), suggesting that these UPLs broadly catalyze polyubiquitination of numerous cellular proteins.

UPLs regulate NPR1 accumulation and SA-induced transcriptional reprogramming

Lack of UPL3 activity is associated with failure to reprogram the transcriptome upon activation of immunity (*19*). Similarly, compared to WT plants, *upl1* and *upl5* mutants were partially defective in SA-induced marker gene expression and transcriptome reprogramming (Fig. 1, A and B, fig. S2A, and table S3). Most SA-induced, UPL-regulated genes were dependent on SA-responsive NPR1 coactivator (fig. S2B) (*19*), suggesting that UPLs may regulate the stability of NPR1. Although NPR1 transcript levels were unaffected, pathogen- and SA-induced accumulation of endogenous NPR1 protein was compromised in all three *upl* mutants (Fig. 1, C and D, and fig. S2C). Reduced accumulation of NPR1 protein was potentially due to decreased SA levels in *upl1* and *upl5* mutants (fig. S2D), as SA is required for NPR1 protein homeostasis (*22*). Mutant *upl3* plants, however, accumulated normal levels of SA (fig. S2D). To investigate this further and to circumvent any effects that were not due to changes in protein stability, we constitutively expressed *NPR1-GFP* (green fluorescent protein) without untranslated regions (UTRs) in *upl npr1-1* double mutants (fig. S2E). In marked contrast to endogenous NPR1, constitutively expressed NPR1-GFP protein accumulated in all *upl* mutants (fig. S2F). As *NPR1-GFP* was expressed without UTRs, these findings may suggest that *upl3* mutants exhibit decreased translation of endogenous NPR1 mRNA, but this remains to be investigated further. Although expression of *NPR1-GFP* restored SA-induced expression of *PR1* (direct NPR1 target gene) in *upl1* and *upl5* mutants, higher levels of NPR1-GFP protein were required compared to the WT background (Fig. 1E and fig. S2F). More notably, NPR1-GFP largely failed to induce *PR1* gene expression in *upl3* mutants (Fig. 1E). These data imply that UPLs, and particularly UPL3, may regulate NPR1's TA activity.

Proteasome-associated UPLs clear transcriptionally inactive NPR1 from target promoters

To explore the possibility that UPLs regulate NPR1 activity, we assessed first whether UPLs interact with NPR1 in vivo. While we

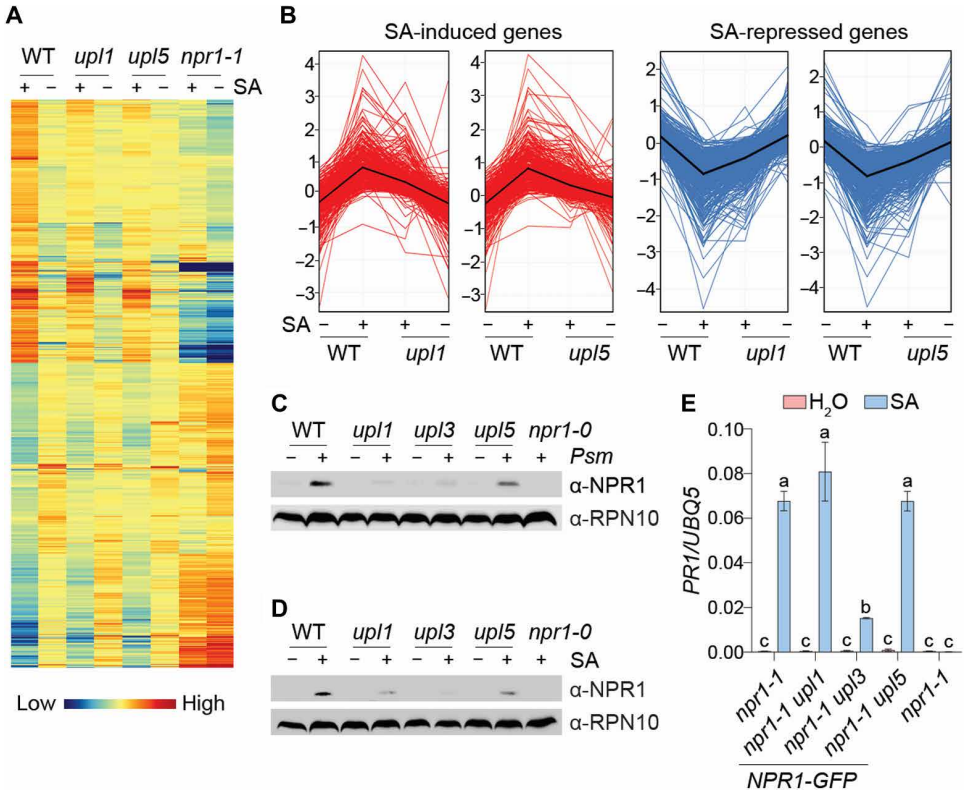

Fig. 1. UPLs are required for SA- and NPR1-dependent transcriptional reprogramming. (**A** and **B**) Mutant *upl* plants are impaired in SA-dependent transcriptional reprogramming. Adult plants were treated with 0.5 mM SA or H_2O for 24 hours, and mRNA was extracted and analyzed by RNA-seq. Genes with fold change of ≥1.5 [Benjamini-Hochberg false discovery rate (FDR), two-way analysis of variance (ANOVA), $P \leq 0.05$, $n = 3$] in WT plants in response to SA are shown as a heatmap (A) and profile plot (B). (**C**) Pathogen-induced accumulation of endogenous NPR1 protein is controlled by UPLs. Indicated genotypes were inoculated with or without *Pseudomonas syringae* pv. *maculicola* ES4326 (*Psm*) (10^6 colony-forming units/ml) and endogenous NPR1 protein detected by immunoblotting, while RPN10 was used as a loading control. (**D**) SA-induced accumulation of endogenous NPR1 protein is controlled by UPLs. Indicated genotypes were treated with 0.5 mM SA or H_2O for 24 hours, and proteins were detected as in (C). (**E**) NPR1-mediated *PR1* gene expression is impaired in *upl3* plants. Seedlings constitutively expressing *NPR1-GFP* in the indicated genetic backgrounds were treated with 0.5 mM SA or H_2O for 6 hours. *PR-1* gene expression was normalized to *UBQ5*. Data represent means ± SD (Tukey post hoc ANOVA test; $\alpha = 0.05$, $n = 3$).

were unable to express UPL1, both epitope-tagged UPL3 and UPL5 coimmunoprecipitated with NPR1-GFP (Fig. 2A). Moreover, the levels of SA-induced polyubiquitinated NPR1-GFP were markedly reduced in *upl* mutants (Fig. 2B). Treatment with the protein synthesis inhibitor, cycloheximide (CHX), demonstrated that while NPR1-GFP was rapidly degraded when expressed in the WT, it was significantly more stable in *upl* mutants (Fig. 2, C and D). Together, these findings show that UPLs polyubiquitinate SA-induced NPR1 and promote its degradation by the proteasome.

Given that UPLs are associated with the proteasome, we reasoned that they might function sequentially after CRL3 and UBE4 ligases to modify NPR1 and promote its degradation. We previously reported that, in contrast to *upl* mutants, mutant *ube4* plants accumulate highly active NPR1 that is modified by short ubiquitin chains (*14*). Therefore, we crossed *ube4* with *upl3* single mutants in an attempt to observe the effect on NPR1's transcriptional activity. Unfortunately, we were unable to obtain homozygous *upl3 ube4* double mutants, suggesting that this combination was lethal. However,

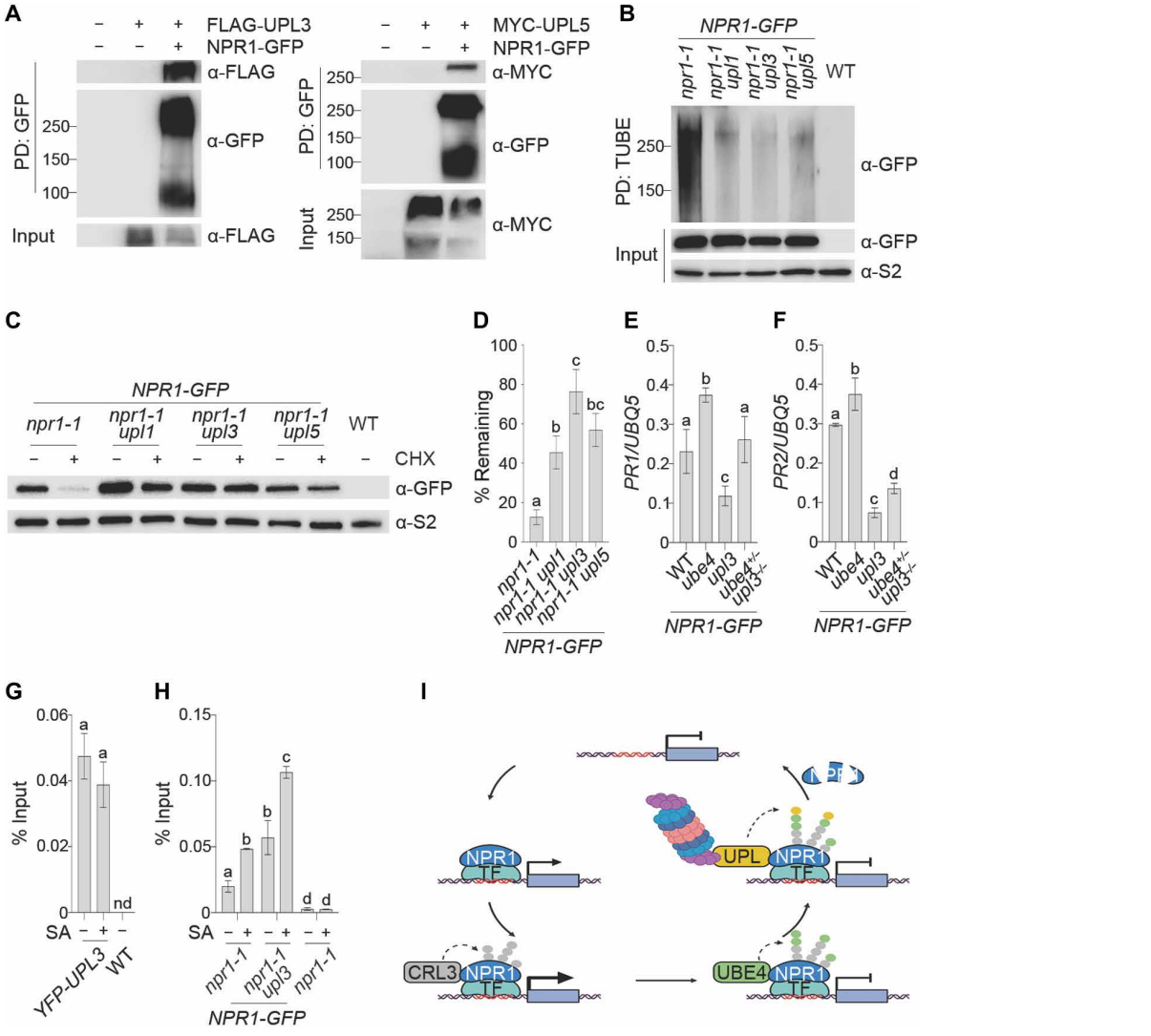

Fig. 2. UPLs polyubiquitinate SA-induced NPR1 and promote its degradation by the proteasome. (**A**) UPLs physically interact with NPR1. NPR1-GFP was transiently expressed with FLAG-UPL3 or MYC-UPL5 in *N. benthamiana*. Protein complexes were pulled down with GFP-Trap agarose and analyzed by immunoblotting against GFP, FLAG, and MYC. (**B**) UPLs polyubiquitinate NPR1. Plants expressing NPR1-GFP were treated for 6 hours with 0.5 mM SA and 100 μM proteasome inhibitor MG132. Ubiquitinated proteins were pulled down with GST-TUBE and analyzed by immunoblotting against GFP and S2 (regulatory non–adenosine triphosphatase subunit RPN1). (**C**) NPR1 is stabilized in *upl* mutants. Plants expressing *pCAB1:NPR1-GFP* were treated with 100 μM CHX or dimethyl sulfoxide vehicle for 2 hours. Proteins were analyzed by immunoblotting against GFP and S2. (**D**) Quantification of remaining NPR1-GFP in (C) (Tukey post hoc ANOVA test; $\alpha = 0.05$, $n = 3$). (**E** and **F**) Mutation of *UBE4* in *upl3* restores *PR* gene expression. Plants expressing NPR1-GFP were treated with 0.5 mM SA for 24 hours. Expression of *PR* genes was normalized to *UBQ5*. Data represent means ± SD (Tukey post hoc ANOVA test; $\alpha = 0.05$, $n = 3$). (**G**) YFP-UPL3 localizes to the *PR-1* promoter. Adult *35S:YFP-UPL3* (*upl3*) plants were treated with 0.5 mM SA or H_2O for 24 hours before assessing YFP-UPL3 binding to the *as-1* motif of the *PR1* promoter. Data represent means ± SD (Tukey post hoc ANOVA test; $\alpha = 0.05$, $n = 3$). nd, not detected. (**H**) NPR1-GFP accumulates at the *PR1* promoter of *upl3* mutants. As in (G), but binding of NPR1-GFP to *PR1* promoter was analyzed. (**I**) CRL3 catalyzes the initiation of ubiquitin chains (gray circles) on promoter-bound NPR1 to enhance its transcriptional output. UBE4-mediated elongation of chains (green circles) results in inactivation of target genes and recruitment of UPL-containing proteasomes. Proteasome-associated UPLs further remodel chains (orange circles) and promote proteasomal degradation and clearance of inactive NPR1 from target promoters. PD, pull-down.

we were able to generate heterozygous knockouts of *UBE4* in mutant *upl3* plants. The *ube4* single, *upl3* single, and $ube4^{+/-}$ $upl3^{-/-}$ double mutants all accumulated higher levels of NPR1-GFP compared to WT (fig. S2, G and H). However, when crossed together, the $ube4^{+/-}$ and $upl3^{-/-}$ mutations did not have observable additive effects on NPR1-GFP protein levels. This was possibly due to the consistently lower (although not significant) expression of *NPR1-GFP* mRNA in the double compared to the single mutants (fig. S1G) or conceivably because additional E3 ligases and deubiquitinases compete to regulate NPR1 protein levels (*12*, *14*, *15*). In addition, compared to WT, the double mutant also exhibited reduced polyubiquitination of NPR1-GFP (fig. S2I), but the pattern of polyubiquitination changed slightly, suggesting that there may be an interplay between UBE4- and UPL3-dependent polyubiquitination of NPR1. Although $ube4^{+/-}$ heterozygotes did not show significantly altered expression of immune genes (fig. S2, J and K), heterozygous knockout of *UBE4* in *upl3* mutants largely restored NPR1's ability to activate *PR1* and *PR2* gene expression (Fig. 2, E and F). These results are in agreement with NPR1 being modified by a ubiquitin ligase relay consisting of CRL3, UBE4, and ending with UPL3.

Our data show that although *upl3* mutants fail to degrade NPR1, they are compromised in SA-induced expression of *PR1*. To understand how UPL3-mediated ubiquitination of NPR1 may influence its TA activity, we assessed chromatin association of both UPL3 and NPR1. UPL3 was constitutively associated with the *PR1* promoter independent of SA treatment (Fig. 2G). By contrast, when expressed in the *npr1-1* mutant background, NPR1-GFP was recruited to the *PR1* promoter only in response to SA treatment. Unexpectedly, however, NPR1-GFP accumulated to much higher levels at the *PR1* promoter of *upl3 npr1-1* double mutants both before and particularly after SA treatment (Fig. 2H). Collectively, these findings show that proteasome-associated UPL3 is the last in a relay of three ubiquitin ligases that polyubiquitinate NPR1 and ensures that transcriptionally inactive NPR1 is cleared from target gene promoters by the proteasome.

An $SCF^{EBF1/2}$-UPL3/4 ubiquitin ligase relay is required for proteasomal processing of EIN3

We then asked whether it is a general phenomenon that unstable TAs are subjected to ubiquitin ligase relays that end in their ubiquitination by proteasome-associated UPLs. Previous studies suggest that some ubiquitin ligases, including hormone-responsive ones, can associate with the proteasome (*23*–*26*). Thus, it is plausible that these ubiquitin ligases physically relay substrates to UPLs and the proteasome.

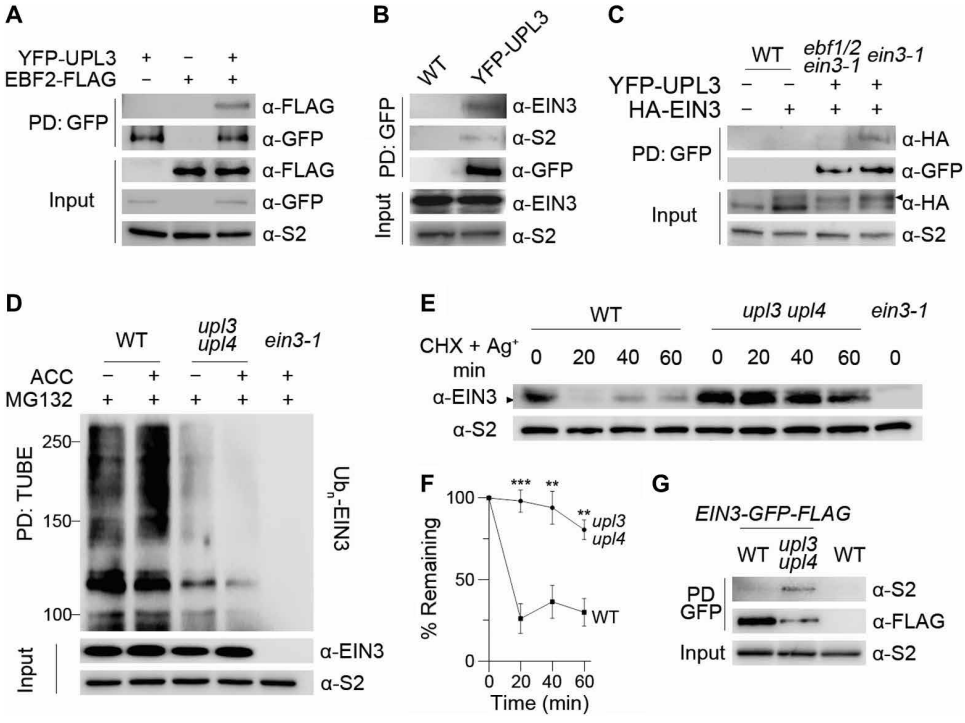

Fig. 3. An $SCF^{EBF1/2}$-UPL3/4 ubiquitin ligase relay is required for proteasomal processing of EIN3. (**A**) UPL3 interacts with EBF2. YFP-UPL3 was purified from *35S:YFP-UPL3* plants with GFP-Trap and incubated with in vitro synthesized FLAG-EBF2. Immunoprecipitated proteins were analyzed by immunoblotting against GFP and FLAG. (**B**) UPL3 interacts with EIN3. Proteins from *35S:YFP-UPL3* (*upl3*) seedlings were pulled down with GFP-Trap and analyzed by immunoblotting against EIN3, GFP, and S2 (loading control). (**C**) UPL3-EIN3 interaction is dependent on EBF1/2. *35S:YFP-UPL3* (*ein3-1*) and *35S:YFP-UPL3* (*ebf1 ebf2 ein3-1*) protoplasts were transformed with *35S:HA-EIN3*. Proteins were pulled down with GFP-Trap and analyzed by immunoblotting against HA, GFP, and S2 (loading control). (**D**) UPL3/4 polyubiquitinates EIN3. Seedlings were treated with 100 μM MG132 and 50 μM ACC for 3 hours. Ubiquitinated proteins were pulled down with His-TUBE and analyzed by immunoblotting against EIN3 and S2 (loading control). (**E**) EIN3 is stabilized in *upl3 upl4* mutants. Seedlings were submerged in 50 μM ACC for 3 hours and then transferred to a combination of 100 μM CHX and 100 μM $AgNO_3$ for the indicated times. Proteins were analyzed by immunoblotting against EIN3 and S2 (loading control). (**F**) EIN3 protein levels were quantified from (E) by normalizing to the levels of S2 protein. Data represent the mean ± SD (two-tailed *t* test, $^{**}P \leq 0.01$; $^{***}P \leq 0.001$; $n = 3$). (**G**) Proteasomal degradation of EIN3 stalls at *upl3 upl4* proteasomes. Proteins from plants expressing *pEIN3:EIN3-eGFP-3xFLAG* in WT and *upl3 upl4* backgrounds were pulled down with GFP-Trap and analyzed by immunoblotting against S2 and FLAG.

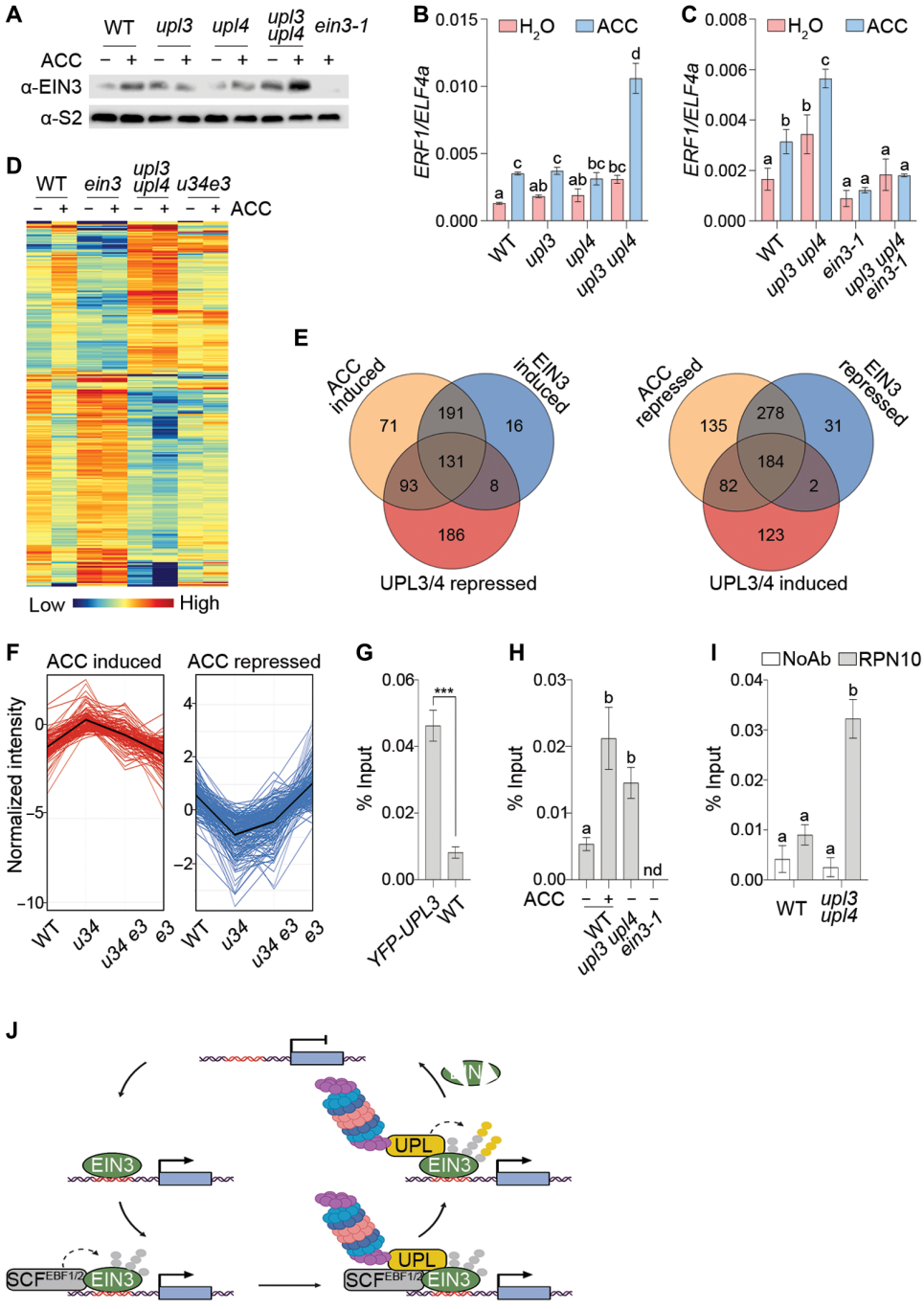

Fig. 4. UPL3/4 is required for EIN3-mediated transcriptional reprogramming. (**A**) Mutant *upl3 upl4* plants accumulate EIN3. Seedlings were treated with 50 μM ACC (3 hours), and proteins were analyzed by immunoblotting against EIN3 and S2. (**B** and **C**) Mutant *upl3 upl4* plants exhibit enhanced expression of an EIN3 target gene. Seedlings were treated as in (A) and levels of *ERF1* expression normalized against *ELF4a*. Data represent means ± SD (Tukey post hoc ANOVA test; $\alpha = 0.05$, $n = 3$). (**D**) Mutant *upl3 upl4* plants display constitutive ethylene-responsive gene expression. Seedlings were treated with 50 mM ACC or H_2O (3 hours) and, mRNA was analyzed by RNA-seq. ACC-responsive genes regulated by both UPL3/4 and EIN3 are shown (fold change ≥ 1.5, Benjamini-Hochberg FDR, two-way ANOVA, $P \leq 0.05$, $n = 3$). (**E**) Venn diagrams of overlaps between ACC-regulated genes, EIN3-regulated genes, and UPL3/4-regulated genes. (**F**) Profile plot of genes in (D). (**G**) UPL3 localizes to the ethylene-responsive *ERF1* promoter. *35S:YFP-UPL3* (*upl3*) plants were analyzed by ChIP with a GFP antibody. Data represent means ± SD (two-tailed *t* test, $^{***}P \leq 0.001$, $n = 3$). (**H**) EIN3 accumulates at the *ERF1* promoter of *upl3 upl4* mutants. Seedlings were treated with 50 μM ACC or H_2O (3 hours) before assessing EIN3 binding to the *ERF1* promoter. Letters indicate statistical differences (Tukey post hoc ANOVA test; $\alpha = 0.05$, $n = 3$). (**I**) Proteasomes accumulate at the *ERF1* promoter of *upl3 upl4* mutants. Seedlings were analyzed by ChIP with an RPN10 proteasome subunit antibody. Data were analyzed as in (H). NoAb, no antibody-negative control. (**J**) Occupancy of EIN3 at ethylene-responsive promoters triggers the expression of target genes. When ethylene levels decrease, $SCF^{EBF1/2}$ catalyzes the ubiquitination (gray circles) of promoter-bound EIN3. Next, EIN3 is physically relayed from $SCF^{EBF1/2}$ to proteasome-associated UPLs, which further remodel EIN3-attached ubiquitin chains (orange circles), thereby promoting its processive degradation by the proteasome.

In agreement with this, we previously found by yeast two-hybrid that the UPL3 N terminus interacts with the F-box protein EBF2, the substrate adaptor protein of an ethylene-responsive $SCF^{EBF1/2}$ ligase that targets the TA EIN3 for degradation (*19*). First, we verified by coimmunoprecipitation that physical interaction between full-length UPL3 and EBF2 indeed takes place in plants (Fig. 3A). Moreover, we found that along with a proteasome regulatory subunit, endogenous EIN3 also coimmunoprecipitated with UPL3 (Fig. 3B). To investigate whether $SCF^{EBF1/2}$ might deliver EIN3 to UPL3 for further ubiquitination, we compared the interaction between hemagglutinin (HA)–tagged EIN3 and yellow fluorescent protein (YFP)–tagged UPL3 in the presence or absence of EBF1 and EBF2. Notably, interaction between HA-EIN3 and YFP-UPL3 was completely dependent on EBF1/2 (Fig. 3C), indicating that $SCF^{EBF1/2}$ is required for EIN3 to be recruited to UPL3 in a previously unknown physical relay.

So why are TAs relayed from pathway-specific ubiquitin ligases to proteasome-associated UPLs? It is plausible that UPLs add or remodel ubiquitin chains on TAs to ensure that they retain high affinity for the proteasome while being degraded. In agreement, regardless of treatment with the ethylene precursor 1-aminocyclopropane 1-carboxylic acid (ACC), polyubiquitination of endogenous EIN3 was markedly reduced when proteasome activity was blocked in a double-knockout mutant of both *UPL3* and its closest homolog *UPL4* (Fig. 3D). We then assessed whether this led to changes in EIN3 stability in *upl3 upl4* mutants. Seedlings were first treated with ACC to allow accumulation of EIN3, after which destabilization of EIN3 was triggered by treatment with silver ions, a potent inhibitor of ethylene action (*27*), as well as the protein synthesis inhibitor CHX. While EIN3 was degraded within minutes of treatment in the WT, it was much more stable in *upl3 upl4* mutants (Fig. 3, E and F). To investigate the effect of UPL3/4-mediated EIN3 polyubiquitination on the proteasome, we expressed epitope-tagged EIN3 in WT and *upl3 upl4* plants (fig. S3A) and assessed its association with the proteasome via the regulatory subunit RPN1 (S2) that is located at the base of the 19*S* particle (*28*). Because of continuous EIN3 degradation, interaction between EIN3 and the proteasome was only barely detectable in WT plants (Fig. 3G). By contrast, EIN3 accumulated at proteasomes in *upl3 upl4* mutants, indicating that its proteasomal degradation was stalled (Fig. 3G). From these experiments, we draw two conclusions. First, while $SCF^{EBF1/2}$ physically relays EIN3 to UPL3 (Fig. 3C), polyubiquitinated EIN3 can still recruit or be recruited to proteasomes in the absence of UPL3/4 (Fig. 3G), suggesting that interaction with $SCF^{EBF1/2}$ may activate UPL3 to engage with EIN3. Second, relay of EIN3 from $SCF^{EBF1/2}$ to UPL3/4 results in "11th hour" polyubiquitination, which is necessary for its processive degradation by the proteasome.

UPL3/4 controls promoter occupancy and transcriptional reprogramming by EIN3

The proteasome plays an important role in limiting ethylene responses by maintaining low steady-state levels of EIN3 (*8*–*10*). As expected, we found that UPL3/4 contributes to this process, as *upl3 upl4* mutants accumulated high levels of endogenous EIN3 even in the absence of ACC-induced ethylene signaling (Fig. 4A and fig. S3B). Compared to WT, the basal and ACC-induced expression of EIN3 target genes was consequently also enhanced in *upl3 upl4* mutants (Fig. 4B and fig. S3, C and D). We then sought to uncover the developmental effect of UPL3/4-mediated regulation of EIN3 by assessing the "triple response" of etiolated seedlings (*29*). In the presence of active ethylene signaling, dark-grown seedlings display a short, thickened root and hypocotyl with an exaggerated apical hook. Similar to *ebf1 ebf2* mutants that fail to degrade EIN3, *upl3 upl4* mutants displayed a phenotype consistent with constitutive ethylene signaling (fig. S3, E to G). To determine whether this phenotype was dependent on EIN3, we generated *upl3 upl4 ein3* triple mutants. The enhanced expression of EIN3 marker genes observed in *upl3 upl4* double mutants was largely lost in this triple mutant (Fig. 4C and fig. S4, A and B). A similar picture was observed across the entire ACC-responsive transcriptome with mutation of EIN3 dampening transcriptional reprogramming caused by knockout of *UPL3* and *UPL4* (Fig. 4, D to F, and table S4). Consequently, the constitutive ethylene response phenotype of *upl3 upl4* plants was partially lost by mutation of EIN3 (fig. S4, C to E). Residual ethylene signaling was likely due to a notable number of ACC-responsive genes that are independent of EIN3 but regulated by UPL3/4 (Fig. 4E). This suggests that UPL3/4 may also target previously described EIN3-like TAs (*30*).

Last, we explored whether UPL3/4 and the proteasome directly control ethylene-responsive transcription by regulating chromatin-associated EIN3. Transgenic YFP-UPL3 was localized to the promoter of *ERF1*, a direct target gene of EIN3 (Fig. 4G). In WT plants, ACC treatment induced the recruitment of EIN3 to the *ERF1* promoter, while in *upl3 upl4* mutants, EIN3 already accumulated at this promoter even in the absence of ACC (Fig. 4H). Thus, UPL3/4 limits the accumulation of EIN3 at target genes, thereby avoiding their untimely activation. We also found that the proteasome was highly enriched at the *ERF1* promoter of *upl3 upl4* mutants (Fig. 4I), suggesting that stalling of EIN3 degradation traps the proteasome at ethylene-responsive genes.

In summary, we have uncovered a previously unknown relay mechanism by which plant hormone–specific TAs are transmitted between different ubiquitin ligases to control their transcriptional activities. Relays terminate at the proteasome where 11th hour polyubiquitination by HECT-type ligases ensures processive TA degradation. Our data suggest that in at least two cases, TAs are physically handed over from pathway-specific ubiquitin ligases to proteasome-associated HECT-type ligases. Consequently, proteasome-associated HECT-type ligases play an indispensable role in plant hormone–induced transcriptional reprogramming. As HECT-type ligases are bound to proteasomes in a variety of different eukaryotes (*16*, *19*, *31*), ubiquitin ligase relays may be a universal mechanism for proteasome-mediated substrate degradation.

MATERIALS AND METHODS

Plant material growth conditions, hormone treatments, and phenotype analysis

All *Arabidopsis* plants used in this study are in the Columbia-0 (Col-0) background. The *upl1* (SALK_063972), *upl3* (SALK_035524), *upl4* (SALK_040984), *upl5* (SALK_116446), *npr1-0* (SALK_204100), *npr1-1*, *ein3-1*, and *ebf1-1 ebf2-1* mutants and *35S:YFP-UPL3* transgenic lines have been described previously (*9*, *14*, *19*, *32*). The HECT domains of UPL1 (amino acids 3238 to 3681), UPL3 (amino acids 1403 to 1888), and UPL5 (amino acids 444 to 873) were cloned into the pENTR/D-TOPO vector (Invitrogen) and then were recombined into pEarleyGate 104 by LR reaction. The cysteine residues in the HECT domains of UPL1 (amino acid 3648), UPL3 (amino acid 1855), or UPL5 (amino acid 839) were mutated into serine residues

by using a QuikChange Lightning Site-Directed Mutagenesis Kit (Agilent). To generate the *pCAB1:NPR1-GFP* construct, the coding sequence of *NPR1* fused with *GFP* was cloned into the pENTR/D-TOPO vector and subsequently recombined into the pCAB1:GW binary vector by LR reaction (*33*). The *pEIN3:EIN3-eGFP-3xFlag* construct was generated using the pART27 vector backbone (*34*). Briefly, the 35*S* promoter of the expression vector pPILY was replaced with the genomic sequence of *EIN3* using Xho I–Nco I restriction digest (*35*). After insertion of eGFP and Flag coding sequences, the fragment of *EIN3* genomic fusion with eGFP-3xFlag was inserted into binary vector pART27 using Not I restriction digest. All plant materials and vectors used are listed in table S1.

For experiments on adult plants, seeds were germinated under long-day condition (16-hour light/8-hour dark) at 65% humidity and 22°C with light intensity of 70 to 100 μmol m^{-2} s^{-1}. For experiments on seedlings, seeds were washed in 100% ethanol for 5 min, followed by incubation in 10% bleach for 5 min, and then plated on Murashige and Skoog (MS) agar media. All plated seeds were kept at 4°C for 2 to 4 days before moving to the growth chamber.

For SA treatment, 4-week-old adult plants were sprayed with 0.5 mM SA (sodium salicylate; Sigma-Aldrich), while seedlings were immersed in 0.5 mM SA or H_2O. For pathogen inoculation, *Psm* ES4326 was grown in LB media supplemented with 10 mM $MgCl_2$. Cells were collected from the overnight cultures and diluted in 10 mM $MgCl_2$ to an appropriate concentration. Plants were infiltrated with a syringe through the abaxial leaf surface.

For treatment with ACC (Sigma-Aldrich), 10-day-old seedlings were treated with H_2O or 50 μM ACC for 3 hours. For analyzing the triple response, seeds were germinated in the dark on MS media supplemented with or without 10 μM ACC. The hypocotyl and root lengths of 4-day-old seedlings were measured with ImageJ.

Gene expression measurements

Total RNA was extracted as described (*12*), and cDNA was synthesized by using SuperScript II Reverse Transcriptase (Invitrogen) according to the manufacturers' instructions. Quantitative polymerase chain reaction (qPCR) was performed by using PowerUp SYBR Green Master Mix (Applied Biosystems) on a StepOnePlus Real-Time PCR system (Applied Biosystems). Primers used for qPCR are listed in table S2.

For the RNA sequencing (RNA-seq) analysis, total RNA was further purified by using the RNeasy Mini Kit (QIAGEN). The RNA-seq reads were aligned to the *Arabidopsis thaliana* TAIR10 genome using Bowtie. TopHat identified potential exon-exon splice junctions of the initial alignment. Strand NGS software in RNA-seq workflow was used to quantify transcripts. Raw counts were normalized using DESeq with baseline transformation to the median of all samples. Data were then expressed as normalized signal values [i.e., $\log_2$(RPKM) where RPKM is read count per kilobase of exon model per million reads] for all statistical tests and plotting. RNA-seq data have been deposited in Array Express at European Molecular Biology Laboratory-European Bioinformatics Institute (EMBL-EBI) under accession codes E-MTAB-10963 and E-MTAB-10964.

Protein analysis

Liquid nitrogen–frozen plant tissue was ground in protein extraction buffer [50 mM tris-HCl (pH 7.5), 150 mM NaCl, 5 mM EDTA, 0.1% Triton X-100, 0.2% NP-40, *N-p*-tosyl-L-phenylalanine chloromethyl ketone (TPCK; 50 μg/ml), *Nα*-tosyl-L-lysine chloromethyl ketone hydrochloride (TLCK; 50 μg/ml), and 0.6 mM phenylmethylsulfonyl fluoride (PMSF)] unless otherwise stated. Protein extracts were incubated with 1× SDS sample buffer supplemented with 50 mM dithiothreitol (DTT) at 80°C for 10 min and then were separated by SDS–polyacrylamide gel electrophoresis (SDS-PAGE). All the antibodies used are listed in table S1.

Endogenous NPR1 was detected by using anti-NPR1 antibody (Agrisera). For NPR1-GFP degradation assay, 2-week-old seedlings were treated with 100 μM CHX, and samples were collected 2 hours after treatment. NPR1-GFP was detected using an anti-GFP antibody (Roche).

For analyzing accumulation of EIN3, samples were ground in protein extraction buffer containing 62.5 mM tris-Cl (pH 6.8), 3% SDS, 10% glycerol, 0.1% bromophenol blue, protease inhibitors [TPCK (50 μg/ml), TLCK (50 μg/ml), and 0.6 mM PMSF], and 3% 2-mercaptoethanol. The mixture was incubated at 95°C for 5 min. For EIN3 degradation assay, 10-day-old seedlings were pretreated with 50 μM ACC for 3 hours and then transferred into MS liquid media containing 100 μM CHX and 100 μM $AgNO_3$, and samples were collected at indicated time points. Endogenous EIN3 was detected by using a previously described anti-EIN3 antibody (*36*).

Glutathione-*S*-transferase (GST)-tagged TUBE (tandem ubiquitin binding entity) and His-TUBE pull-downs of ubiquitinated substrates were performed as previously described (*14*). Total ubiquitination level was detected by using anti-ubiquitin antibody (anti-ubiquitinylated protein clone FK2, Merck), while ubiquitinated NPR1-GFP and EIN3 were detected by immunoblotting with anti-GFP (Roche) and anti-EIN3 (*36*) antibodies, respectively.

In vitro ubiquitination assays

For purification of YFP-HECT, *Agrobacterium tumefaciens* carrying *35S:YFP-HECT* were collected from the overnight cultures and resuspended in infiltration buffer containing 10 mM $MgCl_2$ and 6-benzyladenine (10 μl/liter) to optical density at 600 nm (OD_{600}) = 0.5. *Nicotiana benthamiana* leaves were infiltrated with this *Agrobacterium* suspension and harvested after 3 days of infiltration. Proteins were extracted in buffer containing 125 mM tris-HCl (pH 7.7), 0.25 mM EDTA, 2.5 mM $MgCl_2$, 5% glycerol, 5 mM adenosine triphosphate (ATP), and protease inhibitors. YFP-HECT was then pulled down by using GFP-Trap agarose (ChromoTek). For purification of the proteasome, 4-week-old *Arabidopsis* plants were ground in extraction buffer and incubated overnight with anti-proteasome S2 antibody (Abcam) at 4°C. Protein complexes were then pulled down by using Protein A–agarose beads (Millipore). In vitro ubiquitination assays were performed by incubating the purified proteins (i.e., YFP-HECT or proteasomes) in 80 μl of reaction buffer [125 mM tris-HCl (pH 7.7), 0.25 mM EDTA, 2.5 mM $MgCl_2$, 5 mM ATP, 1 mM DTT, and 10 μM NSC632836 deubiquitinase inhibitor] supplemented with 0.2 μg of recombinant human E1 enzyme (BioVision), 0.2 μg of recombinant E2 enzyme UbcH5c (Ubiquigent), and 10 μg of recombinant human FLAG-ubiquitin (Boston Biochem) at 30°C for 18 hours with shaking. To terminate the reaction, SDS sample buffer containing 50 mM DTT was added and incubated at 80°C for 10 min before separating proteins by SDS-PAGE.

Protein-protein interaction assays

For detecting interactions between UPLs and NPR1, *Agrobacterium* carrying *35S:FLAG-UPL3*, *35S:MYC-UPL5*, or *35S:NPR1-GFP* constructs

were collected and resuspended in infiltration buffer containing 10 mM $MgCl_2$ and 6-benzyladenine (10 μl/liter) to OD_{600} = 0.3. *N. benthamiana* leaves were infiltrated and collected after 3 days of infiltration. For testing in vivo YFP-UPL3 and EIN3 interaction, *Arabidopsis 35S:YFP-UPL3/upl3* and WT plants were treated with 100 μM *N*-carbobenzyloxy-L-leucyl-L-leucyl-L-leucinal (MG132) for 2 hours. Proteins were extracted as described above after which NPR1-GFP or YFP-UPL3 proteins were pulled down using GFP-Trap agarose (ChromoTek) according to the manufacturer's instructions. Next, samples were heated at 70°C for 15 min in SDS sample buffer supplemented with 50 mM DTT before protein separation by SDS-PAGE and immunoblotting with anti-GFP and anti-EIN3 (*36*) antibodies.

For analysis of interaction between FLAG-EBF2 and YFP-UPL3, YFP-UPL3 was purified with GFP-Trap agarose from plants carrying *35S:YFP-UPL3*. Agarose beads were washed three times with wash buffer [10 mM tris/Cl (pH 7.5), 150 mM NaCl, 0.5 mM EDTA, and protease inhibitors] before incubating in wash buffer containing cell-free synthesized FLAG-EBF2 (*37*) at 4°C for 1 hour with rotation. Beads were washed extensively with wash buffer and then boiled for 10 min in SDS sample buffer containing 50 mM DTT. FLAG-EBF2 was detected by immunoblotting with an anti–FLAG–horseradish peroxidase antibody (Sigma-Aldrich).

For analysis of interaction between EIN3-GFP-FLAG and the proteasome, EIN3-GFP-FLAG was purified with GFP-Trap agarose from the indicated genotypes carrying *pEIN3:gEIN3-eGFP-3xFLAG*. The presence of the proteasome was detected using an S2 antibody (Abcam).

To test whether interaction between UPL3 and EIN3 depends on EBF1/2, 10^6 protoplasts from *35S:YFP-UPL3* (in *ein3*) or *35S:YFP-UPL3* (in *ebf1 ebf2 ein3*) plants were prepared and transformed with 100 μg of pEarleyGate 201/*35S:HA-EIN3* plasmid DNA as described previously (*38*–*40*). Next, proteins were extracted as described above, YFP-UPL3 protein was purified using GFP-Trap agarose, and HA-EIN3 and YFP-UPL3 were detected using anti-HA (Thermo Fisher Scientific) and anti-GFP (Roche) antibodies, respectively.

Plant hormone analysis

SA content was determined according to a previously described method with specified modifications (*41*). Briefly, fresh leaves were ground in liquid nitrogen, and 0.1 g of sample was suspended in 4 ml of extraction buffer [1% (v/v) acetic acid in acetonitrile/water (4:1)] with stable isotope-labeled internal standards. Suspended samples were extracted, centrifuged, and concentrated as described previously (*41*). Samples were purified by solid-phase extraction using Oasis WAX cartridges (Waters Corp., Milford, MA, USA) from which SA was eluted with 3% (v/v) formic acid in acetonitrile. Following evaporation of each fraction, samples were analyzed on an Agilent 1260-6410 Triple Quad LC/MS system (Agilent Technologies Inc., Santa Clara, CA, USA) equipped with a Capcell Pak ADME-HR S2 column (Osaka Soda Co. Ltd., Osaka, Japan).

Chromatin immunoprecipitation

Chromatin immunoprecipitation (ChIP) was performed as described previously but with minor modifications (*42*). A total of 500 mg of tissue was cross-linked with 1% formaldehyde by vacuum infiltration for 15 min at room temperature. Glycine was added to a final concentration of 125 mM to quench the cross-linking reaction, and tissue was vacuum-infiltrated for a further 5 min. Cross-linked tissue was washed three times with ice-cold phosphate-buffered saline before freezing in liquid nitrogen. For analyses, nuclei were isolated and lysed as described (*42*), while sonication was performed using a BioRuptor Plus (Diagenode) for 10 cycles of 30 s on and 30 s off at high power. NPR1-GFP and YFP-UPL3 were immunoprecipitated using an anti-GFP antibody (Abcam); EIN3 was immunoprecipitated using an anti-EIN3 antibody (*36*), and the proteasome was immunoprecipitated with an anti-RPN10 antibody (Abcam). Enrichment at chromatin binding sites was analyzed by qPCR using primers listed in table S2.

Statistical analysis

All statistical analyses were performed as described in the relevant figure legends. Briefly, all graphed data represent means ± SD. Statistical analyses were performed using Student's *t* tests or Tukey post hoc analysis of variance (ANOVA) tests with $\alpha = 0.05$. Gene expression analysis, ChIP analysis, and protein quantification were performed on at least 3 replicas per sample, while bioassays were performed with 15 replicas per sample.

SUPLLEMENTARY MATERIALS

Supplementary material for this article is available at https://science.org/doi/10.1126/sciadv.abn4466

View/request a protocol for this paper from *Bio-protocol*.

REFERENCES AND NOTES

1. R. D. Vierstra, The ubiquitin-26S proteasome system at the nexus of plant biology. *Nat. Rev. Mol. Cell Biol.* **10**, 385–397 (2009).
2. D. R. Kelley, M. Estelle, Ubiquitin-mediated control of plant hormone signaling. *Plant Physiol.* **160**, 47–55 (2012).
3. S. Lumba, S. Cutler, P. McCourt, Plant nuclear hormone receptors: A role for small molecules in protein-protein interactions. *Annu. Rev. Cell Dev. Biol.* **26**, 445–469 (2010).
4. L. Tal, M. X. A. Gil, A. M. Guercio, N. Shabek, Structural aspects of plant hormone signal perception and regulation by ubiquitin ligases. *Plant Physiol.* **182**, 1537–1544 (2020).
5. D. Komander, M. J. Clague, S. Urbé, Breaking the chains: Structure and function of the deubiquitinases. *Nat. Rev. Mol. Cell Biol.* **10**, 550–563 (2009).
6. E. H. G. Adams, S. H. Spoel, The ubiquitin-proteasome system as a transcriptional regulator of plant immunity. *J. Exp. Bot.* **69**, 4529–4537 (2018).
7. K. N. Chang, S. Zhong, M. T. Weirauch, G. Hon, M. Pelizzola, H. Li, S. S. Huang, R. J. Schmitz, M. A. Urich, D. Kuo, J. R. Nery, H. Qiao, A. Yang, A. Jamali, H. Chen, T. Ideker, B. Ren, Z. Bar-Joseph, T. R. Hughes, J. R. Ecker, Temporal transcriptional response to ethylene gas drives growth hormone cross-regulation in Arabidopsis. *eLife* **2**, e00675 (2013).
8. H. Guo, J. R. Ecker, Plant responses to ethylene gas are mediated by $SCF^{EBF1/EBF2}$-dependent proteolysis of EIN3 transcription factor. *Cell* **115**, 667–677 (2003).
9. T. Potuschak, E. Lechner, Y. Parmentier, S. Yanagisawa, S. Grava, C. Koncz, P. Genschik, EIN3-dependent regulation of plant ethylene hormone signaling by two *Arabidopsis* F box proteins: EBF1 and EBF2. *Cell* **115**, 679–689 (2003).
10. J. M. Gagne, J. Smalle, D. J. Gingerich, J. M. Walker, S. D. Yoo, S. Yanagisawa, R. D. Vierstra, Arabidopsis EIN3-binding F-box 1 and 2 form ubiquitin-protein ligases that repress ethylene action and promote growth by directing EIN3 degradation. *Proc. Natl. Acad. Sci. U.S.A.* **101**, 6803–6808 (2004).
11. D. Wang, N. Amornsiripanitch, X. Dong, A genomic approach to identify regulatory nodes in the transcriptional network of systemic acquired resistance in plants. *PLOS Pathog.* **2**, e123 (2006).
12. S. H. Spoel, Z. Mou, Y. Tada, N. W. Spivey, P. Genschik, X. Dong, Proteasome-mediated turnover of the transcription coactivator NPR1 plays dual roles in regulating plant immunity. *Cell* **137**, 860–872 (2009).
13. R. Zavaliev, R. Mohan, T. Chen, X. Dong, Formation of NPR1 condensates promotes cell survival during the plant immune response. *Cell* **182**, 1093–1108.e18 (2020).
14. M. J. Skelly, J. J. Furniss, H. Grey, K. W. Wong, S. H. Spoel, Dynamic ubiquitination determines transcriptional activity of the plant immune coactivator NPR1. *eLife* **8**, e47005 (2019).
15. M. Shen, C. J. Lim, J. Park, J. E. Kim, D. Baek, J. Nam, S. Y. Lee, J. M. Pardo, W. Y. Kim, D. Mackey, D. J. Yun, HOS15 is a transcriptional corepressor of NPR1-mediated gene activation of plant immunity. *Proc. Natl. Acad. Sci. U.S.A.* **117**, 30805–30815 (2020).

16. B. Crosas, J. Hanna, D. S. Kirkpatrick, D. P. Zhang, Y. Tone, N. A. Hathaway, C. Buecker, D. S. Leggett, M. Schmidt, R. W. King, S. P. Gygi, D. Finley, Ubiquitin chains are remodeled at the proteasome by opposing ubiquitin ligase and deubiquitinating activities. *Cell* **127**, 1401–1413 (2006).
17. S. Aviram, D. Kornitzer, The ubiquitin ligase Hul5 promotes proteasomal processivity. *Mol. Cell. Biol.* **30**, 985–994 (2010).
18. B. W. Chu, K. M. Kovary, J. Guillaume, L. C. Chen, M. N. Teruel, T. J. Wandless, The E3 ubiquitin ligase UBE3C enhances proteasome processivity by ubiquitinating partially proteolyzed substrates. *J. Biol. Chem.* **288**, 34575–34587 (2013).
19. J. J. Furniss, H. Grey, Z. Wang, M. Nomoto, L. Jackson, Y. Tada, S. H. Spoel, Proteasome-associated HECT-type ubiquitin ligase activity is required for plant immunity. *PLOS Pathog.* **14**, e1007447 (2018).
20. B. P. Downes, R. M. Stupar, D. J. Gingerich, R. D. Vierstra, The HECT ubiquitin-protein ligase (UPL) family in *Arabidopsis*: UPL3 has a specific role in trichome development. *Plant J.* **35**, 729–742 (2003).
21. L. Huang, E. Kinnucan, G. Wang, S. Beaudenon, P. M. Howley, J. M. Huibregtse, N. P. Pavletich, Structure of an E6AP-UbcH7 complex: Insights into ubiquitination by the E2-E3 enzyme cascade. *Science* **286**, 1321–1326 (1999).
22. Z. Q. Fu, S. Yan, A. Saleh, W. Wang, J. Ruble, N. Oka, R. Mohan, S. H. Spoel, Y. Tada, N. Zheng, X. Dong, NPR3 and NPR4 are receptors for the immune signal salicylic acid in plants. *Nature* **486**, 228–232 (2012).
23. Z. Peng, Y. Shen, S. Feng, X. Wang, B. N. Chitteti, R. D. Vierstra, X. W. Deng, Evidence for a physical association of the COP9 signalosome, the proteasome, and specific SCF E3 ligases in vivo. *Curr. Biol.* **13**, R504–R505 (2003).
24. R. Verma, S. Chen, R. Feldman, D. Schieltz, J. Yates, J. Dohmen, R. J. Deshaies, Proteasomal proteomics: Identification of nucleotide-sensitive proteasome-interacting proteins by mass spectrometric analysis of affinity-purified proteasomes. *Mol. Biol. Cell* **11**, 3425–3439 (2000).
25. M. Schmidt, J. Hanna, S. Elsasser, D. Finley, Proteasome-associated proteins: Regulation of a proteolytic machine. *Biol. Chem.* **386**, 725–737 (2005).
26. D. C. Gemperline, R. S. Marshall, K. H. Lee, Q. Zhao, W. Hu, F. McLoughlin, M. Scalf, L. M. Smith, R. D. Vierstra, Proteomic analysis of affinity-purified 26S proteasomes identifies a suite of assembly chaperones in Arabidopsis. *J. Biol. Chem.* **294**, 17570–17592 (2019).
27. E. M. Beyer, A potent inhibitor of ethylene action in plants. *Plant Physiol.* **58**, 268–271 (1976).
28. J. A. M. Bard, E. A. Goodall, E. R. Greene, E. Jonsson, K. C. Dong, A. Martin, Structure and function of the 26S proteasome. *Annu. Rev. Biochem.* **87**, 697–724 (2018).
29. R. Solano, J. R. Ecker, Ethylene gas: Perception, signaling and response. *Curr. Opin. Plant Biol.* **1**, 393–398 (1998).
30. Q. Chao, M. Rothenberg, R. Solano, G. Roman, W. Terzaghi, J. R. Ecker, Activation of the ethylene gas response pathway in Arabidopsis by the nuclear protein ETHYLENE-INSENSITIVE3 and related proteins. *Cell* **89**, 1133–1144 (1997).
31. J. You, C. M. Pickart, A HECT domain E3 enzyme assembles novel polyubiquitin chains. *J. Biol. Chem.* **276**, 19871–19878 (2001).
32. H. Cao, S. A. Bowling, A. S. Gordon, X. N. Dong, Characterization of an Arabidopsis mutant that is nonresponsive to inducers of systemic acquired-resistance. *Plant Cell* **6**, 1583–1592 (1994).
33. M. Michniewicz, E. M. Frick, L. C. Strader, Gateway-compatible tissue-specific vectors for plant transformation. *BMC. Res. Notes* **8**, 63 (2015).
34. A. P. Gleave, A versatile binary vector system with a T-DNA organisational structure conducive to efficient integration of cloned DNA into the plant genome. *Plant Mol. Biol.* **20**, 1203–1207 (1992).
35. A. Ferrando, R. Farras, J. Jasik, J. Schell, C. Koncz, Intron-tagged epitope: A tool for facile detection and purification of proteins expressed in Agrobacterium-transformed plant cells. *Plant J.* **22**, 553–560 (2000).
36. S. Michaeli, M. Clavel, E. Lechner, C. Viotti, J. Wu, M. Dubois, T. Hacquard, B. Derrien, E. Izquierdo, M. Lecorbeiller, N. Bouteiller, J. De Cilia, V. Ziegler-Graff, H. Vaucheret, G. Galili, P. Genschik, The viral F-box protein P0 induces an ER-derived autophagy degradation pathway for the clearance of membrane-bound AGO1. *Proc. Natl. Acad. Sci. U.S.A.* **116**, 22872–22883 (2019).
37. M. Nomoto, Y. Tada, Cloning-free template DNA preparation for cell-free protein synthesis via two-step PCR using versatile primer designs with short 3'-UTR. *Genes Cells* **23**, 46–53 (2018).
38. F. H. Wu, S. C. Shen, L. Y. Lee, S. H. Lee, M. T. Chan, C. S. Lin, Tape-*Arabidopsis* sandwich - a simpler *Arabidopsis* protoplast isolation method. *Plant Methods* **5**, 16 (2009).
39. S. Kneeshaw, S. Gelineau, Y. Tada, G. J. Loake, S. H. Spoel, Selective protein denitrosylation activity of thioredoxin-h5 modulates plant immunity. *Mol. Cell* **56**, 153–162 (2014).
40. L. L. Hansen, G. van Ooijen, Rapid analysis of circadian phenotypes in Arabidopsis protoplasts transfected with a luminescent clock reporter. *J. Vis. Exp.* **115**, e54586 (2016).
41. T. Matsuura, I. C. Mori, E. Himi, T. Hirayama, Plant hormone profiling in developing seeds of common wheat (Triticum aestivum L.). *Breed Sci.* **69**, 601–610 (2019).
42. A. V. Gendrel, Z. Lippman, R. Martienssen, V. Colot, Profiling histone modification patterns in plants using genomic tiling microarrays. *Nat. Methods* **2**, 213–218 (2005).
43. C. Garcia-Barcena, N. Osinalde, J. Ramirez, U. Mayor, How to inactivate human ubiquitin E3 ligases by mutation. *Front. Cell Dev. Biol.* **8**, 39 (2020).
44. K. W. Earley, J. R. Haag, O. Pontes, K. Opper, T. Juehne, K. Song, C. S. Pikaard, Gateway-compatible vectors for plant functional genomics and proteomics. *Plant J.* **45**, 616–629 (2006).
45. M. Karimi, D. Inze, A. Depicker, GATEWAY vectors for Agrobacterium-mediated plant transformation. *Trends Plant Sci.* **7**, 193–195 (2002).
46. A. Sessions, E. Burke, G. Presting, G. Aux, J. McElver, D. Patton, B. Dietrich, P. Ho, J. Bacwaden, C. Ko, J. D. Clarke, D. Cotton, D. Bullis, J. Snell, T. Miguel, D. Hutchison, B. Kimmerly, T. Mitzel, F. Katagiri, J. Glazebrook, M. Law, S. A. Goff, A high-throughput Arabidopsis reverse genetics system. *Plant Cell* **14**, 2985–2994 (2002).
47. S. D. Yoo, Y. H. Cho, G. Tena, Y. Xiong, J. Sheen, Dual control of nuclear EIN3 by bifurcate MAPK cascades in C_2H_4 signalling. *Nature* **451**, 789–795 (2008).

Acknowledgments: We thank M. Skelly for critically reading the manuscript. **Funding:** This work was supported by the European Research Council (ERC) under the European Union's Horizon 2020 research and innovation program, grant agreement no. 678511 (to S.H.S.), Biotechnology and Biological Sciences Research Council (BBSRC) grant BB/S016767/1 (to S.H.S.), Darwin Trust PhD studentship (to Z.W.), Royal Society International Exchanges grant IEC\R3\170118 (to S.H.S. and Y.T.), SPS Grant-in-Aid for Scientific Research (B) grant 16H05065 (to Y.T.), and Agence Nationale de la Recherche (ANR) grant ANR-10-IDEX-0002 and IMCBio ANR-17-EURE-0023 (to T.P. and P.G.). **Author contributions:** Z.W., B.O.-P., and S.H.S. designed the research. Z.W. and B.O.-P. performed experiments. T.P. and P.G. provided crucial research materials. M.N. and T.M. performed hormone quantifications. H.G., I.C.M., Y.T., P.G., and S.H.S. performed project administration and acquired funding. The manuscript was written by Z.W., B.O.-P., and S.H.S. and further edited by T.P. and P.G. **Competing interests:** The authors declare that they have no competing interests. **Data and materials availability:** All data are available in the main text or the Supplementary Materials except for RNA-seq data, which have been deposited in Array Express at EMBL-EBI under accession codes E-MTAB-10963 and E-MTAB-10964. The materials can be provided by S.H.S. pending scientific review and a completed material transfer agreement. Requests for the materials should be submitted to S.H.S.

Submitted 26 November 2021
Accepted 1 September 2022
Published 21 October 2022
10.1126/sciadv.abn4466